Neutron Star Astrophysics at the Crossroads: Magnetars and the Multimessenger Revolution
Proceedings IAU Symposium No. 363, 2023
E. Troja & M. G. Baring, eds.
doi:10.1017/S1743921322000850

Modeling kilonova emission from neutron star mergers

Masaomi Tanaka[1], Daiji Kato[2,3], Gediminas Gaigalas[4], Kyohei Kawaguchi[5], Laima Radžiūtė[4], Pavel Rynkun[4], Smaranika Banerjee[1] and Nanae Domoto[1]

[1]Astronomical Institute, Tohoku University, Sendai 980-8578, Japan
email: masaomi.tanaka@astr.tohoku.ac.jp

[2]National Institute for Fusion Science, 322-6 Oroshi-cho, Toki 509-5292, Japan

[3]Interdisciplinary Graduate School of Engineering Sciences, Kyushu University, Kasuga, Fukuoka 816-8580, Japan

[4]Institute of Theoretical Physics and Astronomy, Vilnius University, Saulėtekio Ave. 3, Vilnius, Lithuania

[5]Institute for Cosmic Ray Research, The University of Tokyo, 5-1-5 Kashiwanoha, Kashiwa, Chiba 277-8582, Japan

Abstract. Coalescence of binary neutron stars gives rise to kilonova, thermal emission powered by radioactive decays of newly synthesized r-process nuclei. Observational properties of kilonova are largely affected by bound-bound opacities of r-process elements. It is, thus, important to understand atomic properties of heavy elements to link the observed signals with nucleosynthesis of neutron star mergers. In this paper, we introduce the latest status of kilonova modeling by focusing on the aspects of atomic physics. We perform systematic atomic structure calculations of r-process elements to understand element-to-element variation in the opacities. We demonstrate that the properties of the atomic structure of heavy elements are imprinted in the opacities of the neutron star merger ejecta and consequently in the kilonova light curves and spectra. Using this latest opacity dataset, we briefly discuss implications for GW170817, expected diversity of kilonova emission, and prospects for element identification in kilonova spectra.

Keywords. radiative transfer, opacity, stars: neutron

1. Introduction

Observations of gravitational waves (GWs) from the neutron star (NS) merger event GW170817 and its electromagnetic counterpart (AT2017gfo, Abbott et al. 2017) opened a new way to study the origin of heavy elements in the Universe. Observed properties of AT2017gfo are largely consistent with theoretically expected "kilonova", thermal emission powered by radioactive decays of newly synthesized r-process elements (e.g., Li & Paczyński 1998; Kulkarni 2005; Metzger et al. 2010). This agreement indicates that r-process synthesis takes place in the NS merger (e.g., Kasen et al. 2017; Tanaka et al. 2017; Perego et al. 2017; Rosswog et al. 2018).

However there remain several key questions, such as (i) which elements are produced, (ii) what kind of ejecta structure reproduces the observed blue (optical) and red (near infrared) components in AT2017gfo, and (iii) what is the diversity of the kilonova properties depending on the masses and mass ratios of merging NSs. To address these issues, we need detailed modeling of kilonova emission.

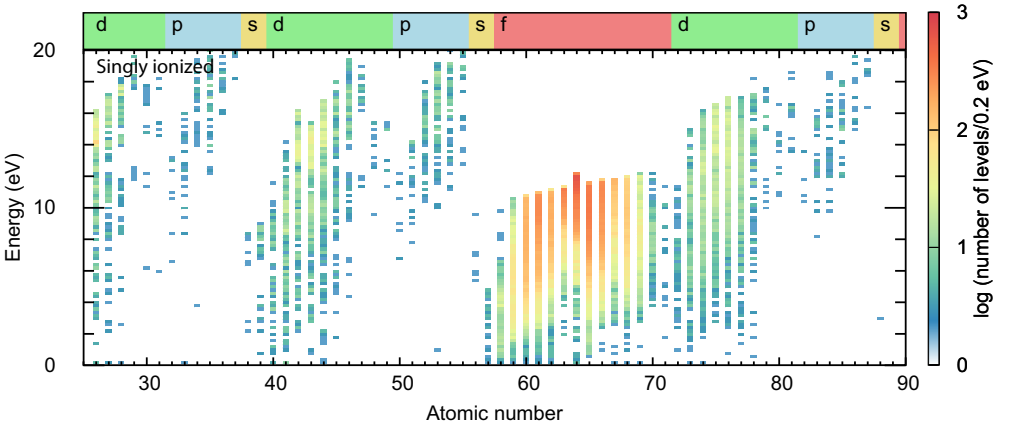

Figure 1. Energy level distribution of singly ionized elements up to the ionization potential. The color scale represents the distribution of energy levels, i.e., the number of energy levels in every 0.2 eV energy bin.

Observational properties of kilonova are affected by several factors (see Rosswog 2015; Fernández & Metzger 2016; Tanaka 2016; Metgzer 2017 for reviews) including macroscopic properties of the ejecta such as the mass and velocity of the ejecta as well as the multi-dimensional structure (Perego et al. 2017; Kawaguchi et al. 2018; Kawaguchi et al. 2020a; Dietrich et al. 2021) and microscopic properties of r-process nuclei and atoms/ions in the ejecta such as radioactive heating rates (e.g., Lippuner, & Roberts 2015; Wanajo 2018; Barnes et al. 2021), thermalization processes of γ-rays, β and α particles, and fission fragments (Barnes et al. 2016), and the atomic opacity in the ejecta. In particular, the atomic opacity plays an important role to shape the spectra of kilonovae and their time evolution because thermal photons gradually escape from the ejecta by interacting with r-process elements via bound-bound transitions. In other words, observations of kilonovae provide important clues of r-process nucleosynthesis in the NS mergers (e.g., Metzger & Fernández 2014; Kasen et al. 2015; Tanaka et al. 2018; Wollaeger et al. 2018).

However, available atomic data for the opacity have been limited, which makes direct comparison between theory and observations challenging. To improve this situation, several efforts have been undertaken to construct the atomic opacities of heavy elements (Kasen et al. 2013; Kasen et al. 2017; Tanaka et al. 2018; Wollaeger et al. 2018; Fontes et al. 2020). Recently, we perform the systematic atomic structure calculations of r-process elements for the first time (Tanaka et al. 2020). This provides the most systematic opacity set for the NS mergers. In this paper, we discuss the latest status of kilonova modeling by focusing on the aspects of atomic physics.

2. Atomic structure and opacity

Atomic structure.

We perform systematic atomic calculations for the elements from Fe ($Z = 26$) to Ra ($Z = 88$) using HULLAC (Hebrew University Lawrence Livermore Atomic Code, Bar-Shalom et al. 2001). Our calculations cover neutral atom and singly to triply ionized states. These ionization stages are typical in the NS merger ejecta at about 1 day after the merger (a typical temperature in the ejecta is $T \sim 10,000$ K).

Figure 1 shows the energy level distribution for singly ionized ions. Although the energy levels are calculated even beyond the ionization potential, we only show the levels below the ionization potential. The color scale represents the distribution of energy levels, i.e.,

https://doi.org/10.1017/S1743921322000850 Published online by Cambridge University Press

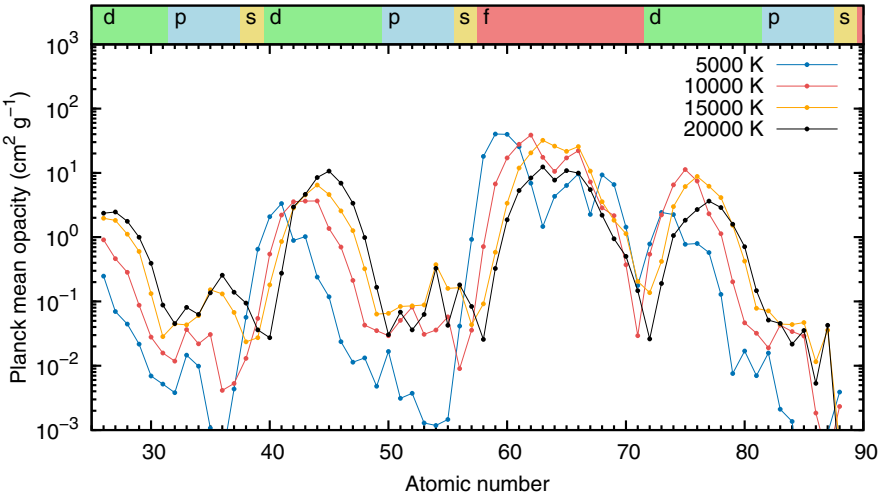

Figure 2. Planck mean opacity at $T = 5,000$ K (blue), 10, 000 K (red), 15, 000 K (orange), and 20, 000 K (black).

the number of energy levels in every 0.2 eV energy bin. We identify the following two effects that mainly determine the energy level distribution.

(1) Within a certain electron shell, the distribution of the energy levels tends to be shifted toward higher energy as more electrons occupy the shell (e.g., $Z = 40$-48 for the case of $4d$ shell and $Z = 57$-71 for the case of $4f$ shell). This is due to the larger energy spacing caused by larger effects of spin-orbit and electron-electron interactions.

(2) At the same time, the number of states is the largest for the half-closed shell since it gives the highest complexity (see also Kasen et al. 2013; Fontes et al. 2020). This effect is most pronounced in the lanthanide elements. For the lanthanide elements with a high complexity, such as Eu ($Z = 63$) and Gd ($Z = 64$), the distribution of the energy levels is pushed up, and thus, the number of low-lying levels is not necessarily higher than that of other lanthanide elements.

Opacity of each element.

Using these results, we calculate the bound-bound opacity for each element (Figure 2). To evaluate the bound-bound opacity for a certain wavelength grid $\Delta\lambda$, we adopt the expansion opacity formalism (Karp et al. 1977; Eastman & Pinto 1993; Kasen et al. 2006):

$$\kappa_{\rm exp}(\lambda) = \frac{1}{ct\rho}\sum_l \frac{\lambda_l}{\Delta\lambda}(1 - e^{-\tau_l}), \tag{2.1}$$

where the summation is taken over all the transitions within the wavelength bin $\Delta\lambda$. The optical depth of one bound-bound transition is evaluated by Sobolev optical depth τ_l (Sobolev 1960), which is a sound approximation in the expanding ejecta with a large velocity and a large velocity gradient. We assume local thermodynamic equilibrium (LTE) for the calculations of ionization and excitation to evaluate the Sobolev optical depth of each transition.

According to the atomic property (1) above, the elements with a fewer number of electrons in the outermost shells tend to give larger contributions to the bound-bound opacities in particular at a lower temperature (see the blue line in Figure 2) because such elements have more low-lying energy levels. Although the opacity of Fe (well-studied for

https://doi.org/10.1017/S1743921322000850 Published online by Cambridge University Press

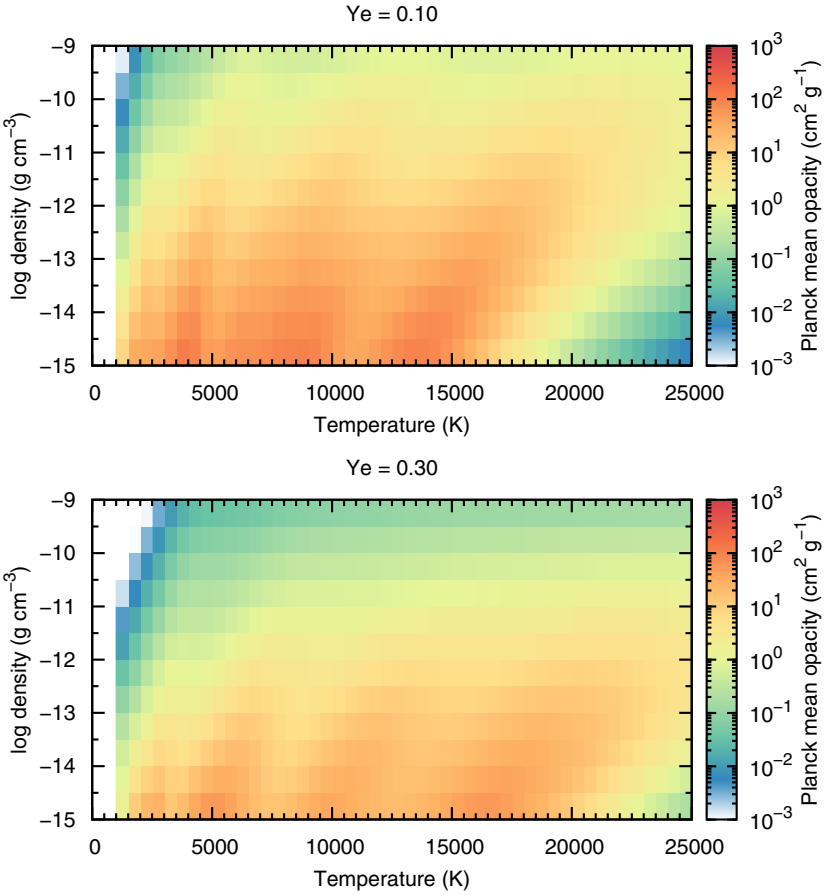

Figure 3. Planck mean opacities for the element mixture ($Y_e = 0.10$ and $Y_e = 0.30$).

supernovae) have been assumed for the opacity of lanthanide-free ejecta from NS mergers, our results imply that Fe is not representative for the opacities of light r-process elements.

Also, by the atomic property (2) above, among lanthanide elements, the most complicated elements, such as Eu ($Z = 63$) or Gd ($Z = 64$), do not necessarily show higher opacities than those of other lanthanide elements in a low temperature (see also Fontes et al. 2020). As the temperature becomes higher, the opacities tend to follow the complexity as the population of the excited states increases (see the black line in Figure 2).

Opacity of the element mixture.

NS merger ejecta include many r-process elements and the abundance distribution is mainly determined by an electron fraction Y_e. The systematic atomic data presented above enable us to connect the abundance pattern (or electron fraction Y_e) with the atomic opacities. For typical physical conditions of kilonova, i.e., $T = 5,000 - 10,000$ K, $\rho = 1 \times 10^{-13}$ g cm^{-3}, and $t = 1$ day after the merger, we wind that the Planck mean opacities for the mixture of r-process elements are $\kappa \sim 20 - 30$ cm^2 g^{-1} for $Y_e \leq 0.20$, $\kappa \sim 3 - 5$ cm^2 g^{-1} for $Y_e = 0.25 - 0.35$, and $\kappa \sim 1$ cm^2 g^{-1} for $Y_e = 0.40$.

It is emphasized that the opacity depends not only on the element abundances, but also on the temperature, density, and time (see Eq. (2.1)). Figure 3 shows the Planck mean opacities at $t = 1$ day for various temperatures and densities in the cases of $Y_e = 0.10$ (lanthanide rich) and 0.30 (lanthanide poor). The large variation in the $\rho - T$ plane

https://doi.org/10.1017/S1743921322000850 Published online by Cambridge University Press

indicates that the opacity in the ejecta is not uniform even for a given time by reflecting the density and temperature structure of the ejecta. Therefore, the detailed modeling including these dependence is required to connect the observed properties and the element abundances.

Our atomic data are publicly available in the Japan-Lithuania Opacity Database for Kilonova † (Kato et al. 2021) in the database of National Institute of Fusion Science (NIFS). The database includes all the energy levels and radiative transitions from our systematic atomic calculations. Also, Planck mean opacities for several element mixtures are available for a wide range of the temperature, density, and time.

3. Discussion

Kilonova modeling.

Our new opacity set gives a reliable link between theory and observations. Using the dataset, Kawaguchi et al. (2018) and Kawaguchi et al. (2020a) performed multi-dimensional radiative transfer simulations for AT2017gfo. For AT2017gfo, the presence of both red and blue components is confirmed from the observed data. Overall, this is consistent with a theoretical picture where lanthanide-rich dynamical ejecta give rise to the red component and lanthanide-poor post-merger ejecta result in the blue component. However, the estimated ejecta parameters for these components are not necessarily consistent with the theoretical expectations. Namely, the ejecta mass of the red component ($M_{\rm ej} \sim 0.03\ M_\odot$) is too massive to be interpreted as the dynamical ejecta while the velocity of the red component ($v \sim 0.2\ c$) is too fast compared with that of the post-merger ejecta.

Multi-dimensional simulations by Kawaguchi et al. (2018, 2020a) highlight the importance of the interplay between two ejecta components. They assume relatively massive, slower post-merger ejecta surrounded by less massive, faster dynamical ejecta, as expected from numerical relativity simulations. In such a configuration, bluer photons originated from the post-merger ejecta are reprocessed by the outer dynamical ejecta, which results in the red kilonova component (see also Dietrich et al. 2021). The calculated light curves give a nice agreement with those of AT2017gfo (Figure 4). Although this model may not be a unique solution to reproduce the observed properties of AT2017gfo, future observations of NS mergers from different viewing angles will constrain the multi-dimensional ejecta structure.

Toward future multi-messenger observations, it is also important to understand the variety of kilonova properties, depending on the NS masses and mass ratios. We refer the readers to Kawaguchi et al. (2020a) for the expected diversity of kilonova as well as Kawaguchi et al. (2021) for a dedicated study of low-mass NS mergers and Kawaguchi et al. (2020b) for black hole-NS mergers. These scenarios can be tested by future observations and also by a variety of kilonova candidates associated with short gamma-ray bursts (e.g., Gompertz et al. 2018; Ascenzi et al. 2019; Rossi et al. 2020; Rastinejad et al. 2021).

Future prospects.

Although modeling of kilonova has been improved in the past several years, there is room for further improvement for more realistic modeling. Here we discuss the current limitation and future prospects by focusing on atomic physics aspects.

A obvious limitation is that most of the current atomic data have been constructed for low ionization states (up to third or fourth ionization), which are appropriate in the NS merger ejecta only after $t \sim 1$ day. Thus, it has been challenging to provide quantitative prediction for earlier kilonova emission. Recently, Banerjee et al. (2020) constructed the

† http://dpc.nifs.ac.jp/DB/Opacity-Database/

https://doi.org/10.1017/S1743921322000850 Published online by Cambridge University Press

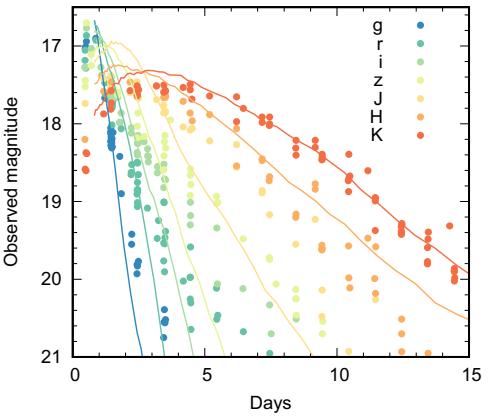

Figure 4. Light curves of GW170817/AT2017gfo compared with the results of multi-dimensional radiative transfer simulations (Kawaguchi et al. 2018; Kawaguchi et al. 2020a)

atomic data for higher ionization states (up to 10th ionization) for the elements up to Ba (Z = 56). They showed that their blue kilonova model can naturally explain the observed early emission in AT2017gfo. Atomic data of highly ionized lanthanides are also being constructed (Carvajal Gallego et al. 2022; Banerjee et al. 2022 in this volume). Such works will enable the calculations of early emission also from the lanthanide-rich ejecta, which may be tested by future observations of NS mergers viewed from the equatorial direction.

It is also important to assess the accuracy of the opacities. Several *ab-initio* atomic calculations have been performed for selected lanthanides in different ionization states (Gaigalas et al. 2019; Carvajal Gallego et al. 2021) and a series of lanthanides for a particular ionization state (Radžiūtė et al. 2020; Radžiūtė et al. 2021). They typically reach the accuracy of as good as ~ 10 % in the energy levels, as compared with the experimentally calibrated data. By these calculations, it is shown that the opacities from systematic atomic calculations agree with those from *ab-initio* calculations within a factor of 1.5-2.0 (Tanaka et al. 2018; Gaigalas et al. 2019).

For conclusive identification of individual elements in NS mergers it is important to decode the spectral features, which requires experimentally calibrated, accurate atomic data. In fact, time series of spectra in the optical and infrared wavelengths have been obtained for AT2017gfo (e.g., Chornock et al. 2017; Kasliwal et al. 2017; Pian et al. 2017; Smartt et al. 2017; Troja et al. 2017). So far, only Sr ($Z = 38$) has been identified in these spectra (Watson et al. 2019; Domoto et al. 2021, see also Perego et al. 2020 and Gillanders et al. 2021 for the constraints on the abundances of He and Au/Pt in the ejecta, respectively). As demonstrated in Domoto et al. (2021), to fully understand the spectral features, accurate transition data in the NIR wavelengths are important as such data are currently highly incomplete.

The spectral features of kilonova not only give element identification but also give important clues of the physical condition of the ejecta. For example, Domoto et al. (2021) show that the Ca lines (mainly ^{48}Ca in neutron-rich environments) can produce strong absorption features in kilonova spectra, as Sr and Ca have a similar atomic structure, i.e., only one s electron when it is singly ionized. The absence of the Ca lines in AT2017gfo, combined with the presence of the Sr lines, gives constraints to Y_e and entropy of the ejecta.

https://doi.org/10.1017/S1743921322000850 Published online by Cambridge University Press

Finally, one of the most unexplored areas is modeling of spectra in the nebular phase. Due to the smaller ejecta mass and higher expansion velocity, kilonovae enter the nebular phase earlier than supernovae. As the emission lines in the nebular phase are centered at the rest wavelength of the transition, we are able to obtain more direct element identification in particular in the inner ejecta. However, since most of the atomic data of heavy elements have been constructed for modeling of the photospheric phase, full atomic data needed for non-LTE modeling are still highly incomplete.

Recently non-LTE modeling of kilonova spectra has just began (Hotokezaka et al. 2021; Pognan et al. 2022). For example, Hotokezaka et al. (2021) showed that the nebular spectra from the pure Nd ejecta exibit a broad structure from optical to infrared wavelengths, with broad peaks around 1 μm and 10 μm. More detailed modeling, with more elements and with accurate atomic data, will provide more quantitative prediction, which can be directly tested by observations with the James Webb Space Telescope (JWST) and upcoming 30 m-class telescopes.

References

Abbott, B. P., et al. 2017, *ApJL*, 848, L12
Ascenzi, S., et al. 2019, *MNRAS*, 486, 672
Bar-Shalom, A., Klapisch, M., & Oreg, J. 2001, *J. Quant. Spectrosc. Radiative Transfer*, 71, 169
Banerjee, S., et al. 2020, *ApJ*, 901, 29
Banerjee, S., et al. 2022, in this volume
Barnes, J. & Kasen, D. 2013, *ApJ*, 775, 18
Barnes, J., Kasen, D., Wu, M.-R., & Martínez-Pinedo, G. 2016, *ApJ*, 829, 110
Barnes, J., et al. 2021, *ApJ*, 918, 44
Carvajal Gallego, H., Palmeri, P., & Quinet, P. 2021, *MNRAS*, 501, 1440
Carvajal Gallego, H., et al. 2022, *MNRAS*, 509, 6138
Chornock, R., et al. 2017, *ApJL*, 848, L19
Dietrich, T., et al. 2021, *Science*, 370, 1405
Domoto, N., Tanaka, M., Wanajo, S., & Kawaguchi, K. 2021, *ApJ*, 913, 26
Eastman, R. G. & Pinto, P. A. 1993, *ApJ*, 412, 731
Fernández R. & Metzger B. D. 2016, *Annual Review of Nuclear and Particle Science*, 66, 23
Fontes, C. J., et al. 2020, *MNRAS*, 493, 4143
Gompertz, B. P., et al. 2018 *ApJ*, 860, 62
Gaigalas, G., et al. 2019, *ApJS*, 240, 29
Gillanders, J. H., et al. 2021, *MNRAS*, 506, 3560
Hotokezaka, K., Tanaka, M., Kato, D., & Gaigalas, G. 2021, *MNRAS*, 506, 5863
Karp, A. H., et al. 1977, *ApJ*, 214, 161
Kasen, D., Thomas, R. C., & Nugent, P. 2006, *ApJ*, 651, 366
Kasen, D., Badnell, N. R., & Barnes, J. 2013, *ApJ*, 774, 25
Kasen, D., Fernández, R., & Metzger, B. D. 2015, *MNRAS*, 450, 1777
Kasen, D., et al. 2017, *Nature*, 551, 80
Kasliwal, M. M., et al. 2017, *Science*, 358, 1559
Kato, D., et al. 2021, Japan-Lithuania Opacity Database for Kilonova (version 1.0)
Kawaguchi, K., Shibata, M., & Tanaka, M. 2018, *ApJL*, 865, L21
Kawaguchi, K., Shibata, M., & Tanaka, M. 2020a, *ApJ*, 889, 171
Kawaguchi, K., Shibata, M., & Tanaka, M. 2020b, *ApJ*, 893, 153
Kawaguchi, K., et al. 2021, *ApJ*, 913, 100
Kulkarni, S. R. 2005, arXiv:2005.10256
Li, L.-X., & Paczyński, B. 1998, *ApJL*, 507, L59
Lippuner, J. & Roberts, L. F. 2015, *ApJ*, 815, 82
Metzger, B. D., et al. 2010, *MNRAS*, 406, 2650
Metzger, B. D., & Fernández, R. 2014, *MNRAS*, 441, 3444
Metzger, B. D. 2017, *Living Reviews in Relativity*, 20, 3

https://doi.org/10.1017/S1743921322000850 Published online by Cambridge University Press

Perego, A., et al. 2017, *ApJL*, 850, L37
Perego, A., et al. 2020, arXiv:2009.08988
Pian, E., et al. 2017, *Nature*, 551, 67
Pognan, Q., Jerkstrand, A., & Grumer, J. 2022, *MNRAS*, 510, 3806
Radžiūtė, L., et al. 2020, *ApJS*, 248, 17
Radžiūtė, L., et al. 2021, *ApJS*, 257, 29
Rastinejad, J. C., et al. 2021, *ApJ*, 916, 89
Rossi, A., et al. 2020, *MNRAS*, 493, 3379
Rosswog S. 2015, *International Journal of Modern Physics D*, 24, 1530012
Rosswog, S., et al. 2018, *A&A*, 615, A132
Smartt, S. J., et al. 2017, *Nature*, 551, 75
Sobolev, V. V. 1960, Moving envelopes of stars
Tanaka, M. & Hotokezaka, K. 2013, *ApJ*, 775, 113
Tanaka, M. 2016, *Advances in Astronomy*, 2016, 634197
Tanaka, M., et al. 2017, *PASJ*, 69, 102
Tanaka, M., et al. 2018, *ApJ*, 852, 109
Tanaka, M., Kato, D., Gaigalas, G., & Kawaguchi, K. 2020, *MNRAS*, 496, 1369
Troja, E., et al. 2017, *Nature*, 551, 71
Wanajo S., et al. 2014, *ApJL*, 789, L39
Wanajo S. 2018, *ApJ*, 868, 65
Watson, D., et al. 2019, *Nature*, 574, 497
Wollaeger, R. T., et al. 2018, *MNRAS*, 478, 3298